UNIMAP
UNIVERSITI MALAYSIA PERLIS

The Effect of SrO doping on LaFeO$_3$ using Yarosite Extraction based Ethanol Gas Sensors Performance Fabricated by Coprecipitation Method

Endi Suhendi[1,a], Muhamad Taufik Ulhakim[1,b], Andhy Setiawan[1,c] and Dani Gustaman Syarif[2,d]

[1]Program Studi Fisika, Universitas Pendidikan Indonesia, Bandung, Indonesia

[2]Pusat Sains dan Teknologi Nuklir Terapan, Badan Tenaga Nuklir Nasional, Bandung, Indonesia

[a]endis@upi.edu, [b]muhamad.taufik.ulhakim@gmail.com, [c]andhys@upi.edu, [d]danigus@batan.go.id

Abstract. Nowadays, semiconductor is one of the most important materials in application of science and technology especially gas sensor. In this present work, characterizing of undoped and doped 10 mol% of SrO on LaFeO$_3$ based ethanol gas sensors has been conducted using LaCl$_3$.7H$_2$O, Fe$_2$O$_3$ from yarosite extraction, and SrCl$_2$.6H$_2$O. The used materials were prepared through coprecipitation method. The ethanol gas sensors were made in the form of thick film using screen printing techniques and fired at 600°C for 2 hours. Characterization of crystal and morphology structures were carried out by using x-ray diffraction (XRD) and scanning electron microscopy (SEM), respectively. Electrical properties of ethanol gas sensors were examined using gas chamber. The XRD analysis indicated that thick films had cubic crystal structure. The SEM analysis showed that doped 10 mol% of SrO decreased the grain size of LaFeO$_3$ from 31.29 nm to 29.56 nm. The analysis of electrical properties showed that the thick film doped by 10 mol% of SrO has a higher response compared to undoped of SrO. The operating temperature of thick films doped by 10 mol% of SrO is 295°C-300°C, this value is lower than the undoped of SrO operating temperature, it's 345 ^{o}C – 355 ^{o}C. Electrical properties indicate that thick film doped by 10 mol% of SrO is the best sensor. These results show that yarosite extraction can be used as the main material in gas sensor fabrication.

Keywords: LaFeO$_3$, yarosite, ethanol gas sensor, SrO doping, coprecipitation method

1. INTRODUCTION

Gas sensor is one of the crucial components used in daily life to detect the harmful gases [1]. One type of gas sensor that is widely used and being developed is a semiconductor based gas sensor or what so-called metal oxide semiconductor [2]. Ethanol is the most common compound that can be extensively used in gas sensor for its practical in various applications such as biomedicine, hospital, safety, food packaging testing, and breath analyzer of drivers which can help to reduce the number of accidents [3]. Some of types of gas sensor have been developed by Sunghoon Park [4], Chang Su [5], LiLi Wang [6], Cheng Wang [7], and Zihua Wang [8].

The metal oxide semiconductor based gas sensor can be made from various materials such as Fe$_2$O$_3$ [9], SnO$_2$ [10], ZnO [11], and LaFeO$_3$ [12]. LaFeO$_3$ is the appropriate material for gas sensor and has a good response to ethanol gases [13-14]. Some impurities can be adding to the main material to get a good response on ethanol gas sensor, it is such as what have been successfully done by Thaweechai using metal-organic decomposition and found out that Sr doping on LaFeO$_3$ produced a good response [15]. The augmentation of doping agent may cause the grain size of the used material to become smaller and according to Zhang (2015) if the grain size is smaller, the response will be better [16].

In this paper, the researchers have synthesized LaFeO$_3$ and LaFeO$_3$ doped by 10 mol% of SrO using coprecipitation method for ethanol gas sensor. The researchers chosing to adding the 10 mol% of SrO as a dopant it based to the result of Thaweechai research which found out that the sensor will get the lower response if the dopant more of 10 mol%. So, the 10 mol% was the proper amount of dopant for improving the ethanol sensing properties on LaFeO$_3$-based sensor [15]. One of the materials that the

International Journal of Nanoelectronics and Materials

In Press, Accepted Manuscript – Note to users

UNIVERSITI
MALAYSIA
PERLIS

UniMAP

researchers used in this study was yarosite extraction and the aim of using yarosite extraction is to found out and prove that natural materials have the good characteristics to applied in gas sensors. The coprecipitation method was employed in this study for the method is favorable to produce smaller grain size or even the nanoparticles [17].

2. MATERIALS AND METHODS

2.1 Preparation of undoped and doped 10 mol% on LaFeO₃ powders

The materials were synthesized by coprecipitation method of $LaCl_3.7H_2O$, Fe_2O_3 from yarosite extraction, and $SrCl_2.6H_2O$. In this study, two material were made. There are the undoped and doped 10 mol% SrO on $LaFeO_3$. The first material is undoped $LaFeO_3$. The material was prepared by mixing the solution of $LaCl_3,7H_2O$, and the solution of Fe_2O_3 from yarosite extraction. The second material is doped with 10 mol% of SrO on $LaFeO_3$. The material was prepared by mixing the solution of $LaCl_3.7H_2O$, the solution of Fe_2O_3 from yarosite extraction and the solution of $SrCl_2.6H_2O$. To prepare both solutions, each material is dissolved in aquadest. To make the solution of Fe_2O_3, the material was dissolved in acid. Then, ammonia hydroxide (NH_4OH 25%) were added to each mixed solutions to produce the precipitate of undoped and doped 10 mol% SrO on $LaFeO_3$. Both precipitate were dried at 100℃ for 6 hours and then calcined at 600℃ for 2 hours and 800℃ for 3 hours. After that, both material respectively are crushed until the material powders are produced.

2.2 Thick film fabrication

Thick films of undoped $LaFeO_3$ and doped 10 mol% SrO on $LaFeO_3$ were fabricated using screen printing techniques. Firstly, the alumina substrate was coated with silver and burned at 600℃ for 10 minutes. Then, the silver coated substrate was coated with a paste of materials and burned at 600℃ for 2 hours. The illustration of the thick film is shown in Figure 1. The paste materials are mixture of the main material powders and organic vehicle. In this study, the mixture consist of 70% main material and 30% organic vehicle.
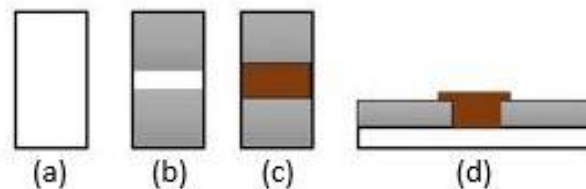

Figure 1. (a) Alumina substrate (b) Alumina substrate coated with silver (c) Alumina substrate which has been coated in silver and coated again with the material paste (d) The thick films were made viewed from the side.

2.3 Characterization of thick films

2.3.1 Structural and morphology characterization

Structural characterizations were carried out using x-ray diffraction (XRD) and scanning electron microscopy (SEM). XRD characterization was done by firing X-ray with Cu $K_\alpha 1$ wavelength $(1,5406 \, x \, 10^{-10}m)$ using PANanalytical X'Pert Pro Series PW3040/x0 X'Pert Pro. From this analysis, the average of crystallites sized and the lattice parameters were found. The average of crystallites sized was calculated using Debye-Scherrer as shown in equation (Eq. 1) [18].

$$D = \frac{0.89\lambda}{B\cos\theta}$$ (1)

where λ is the wavelength of X-ray source and B is the full at half-maximum intensity (FWHM) in radians of a peak at Bragg's angle θ.

SEM characterization was done by Analysis Scanning Electron Microscopy JEOL JSM – 6360LA. From this analysis the grain sized was found by making the comparison of the image scale produced with the benchmark scale of the magnification performed.

2.3.2 Electrical properties

The characterization of electrical properties is conducted to recognize the electrical properties of the thick film of undoped and doped 10 mol% of SrO which applied as ethanol gas sensor. This characterization was performed by measuring the resistance at each 5℃ temperature change under ambient condition (without ethanol) and in the condition of ethanol gas containing. The resistance measurement using the multimeter which connected to the probe in the gas chamber as shown in Figure 2.
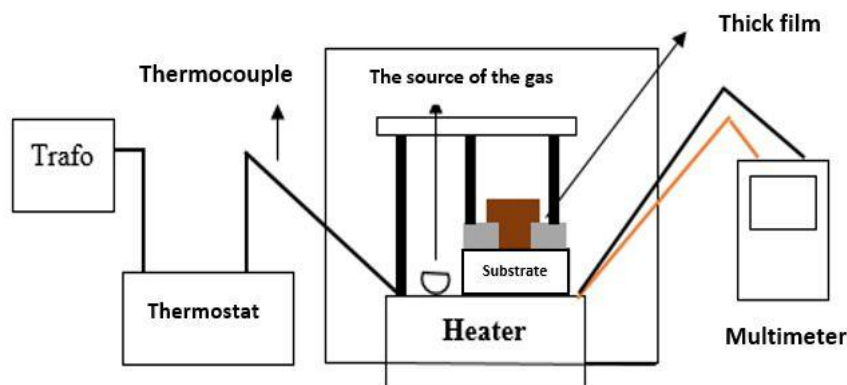

Figure 2 Design of resistance measurement devices.

The results of this characterization were response and operation temperature. That result was obtained from the calculation by using the Equation (Eq. 2) bellow [19-25].

$$Response = \frac{\Delta R}{R_a} = \frac{R_g - R_a}{R_a} \tag{2}$$

where R_g is the resistance of gas sensor that in a test on ethanol containing and R_a is the air resistance of the gas sensor.

3. RESULTS AND DISCUSSION

3.1 Crystal structure and morphology characterizations

The X-ray diffraction (XRD) patterns of undoped $LaFeO_3$ and doped 10 mol% SrO on $LaFeO_3$ are shown in Figure 3. The patterns show that both materials had two phases i.e $LaFeO_3$ as main phase and Fe_2O_3 as second phase. XRD analysis shows that both materials had cubic structure which indicated with (100), (101), (111), (200), (201), (211), (202), and (301) planes, those diffraction data are reffering to JCPDS card of $LaFeO_3$ (JCPDS No. 96-154-2033).
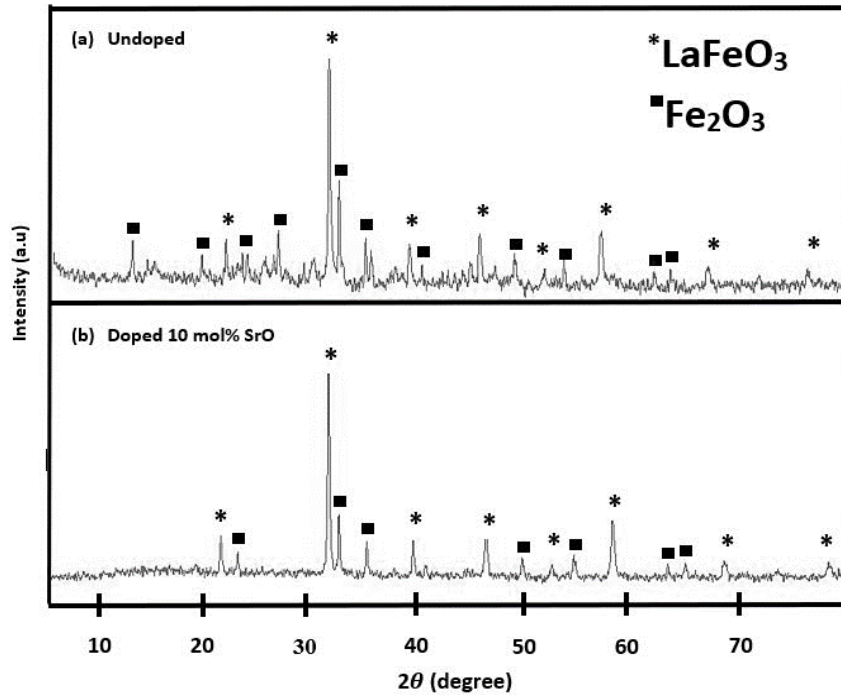
Figure3. XRD pattern of undoped LaFeO$_3$ and doped 10 mol% SrO on LaFeO$_3$ on thick films.

The average of crystallite size has been calculated using Debye-Scherrer's formula as shown in equation 1. It was found that the crytallite size decreased when 10 mol% of SrO is added to the main material.

This study also investigated the average grain size using scanning electron microscopy (SEM) as shown in Figure4. SEM images of undoped LaFeO$_3$ and doped 10 mol% SrO on LaFeO$_3$ were taken in the form of thick films which calcined at 600℃ for 2 hours and 800℃ for 3 hours. In this investigation, it was found that the size of grain decreased when dopant were added to the main material.
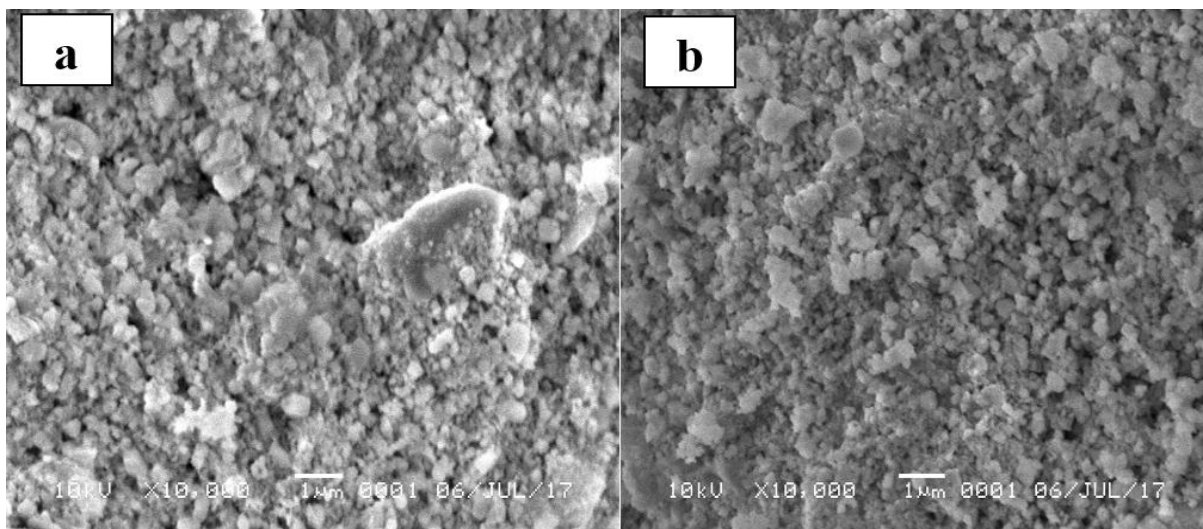

Figure 4. SEM characterization images of (a) undoped and (b) doped 10 mol% SrO on LaFeO$_3$.

Crystallites size and grain size were decreased when 10 mol% of SrO was added on LaFeO$_3$. Its caused Sr^{2+} ion has been successfully to substituted La^{3+} ion on LaFeO$_3$ perfectly. It work because the size of radius ionic of La^{3+} (0.13nm) doesn't have the significant difference with the size of radius ionic of Sr^{2+} (0.14 nm) [26-27]. The results were summarized as shown in Table 1.

Table 1 Structure and morphology characterization results of undoped LaFeO$_3$ and doped 10 mol% SrO on LaFeO$_3$

Compounds	Undoped	Doped 10 mol% SrO
Lattice parameters a = b = c = Å	3.8977	3.9516
Crystallites size D (nm)	31.29	29.56
Grain size (μm)	0.42	0.26

3.2 Electrical properties characterization

Response and operating temperature were two components that influence metal oxide semiconductor gas sensing. In this study, the relation between response and operating temperature was investigated in various gas concentration as shown in Figure 5. The response has been calculated by using the formula shown in equation 2.
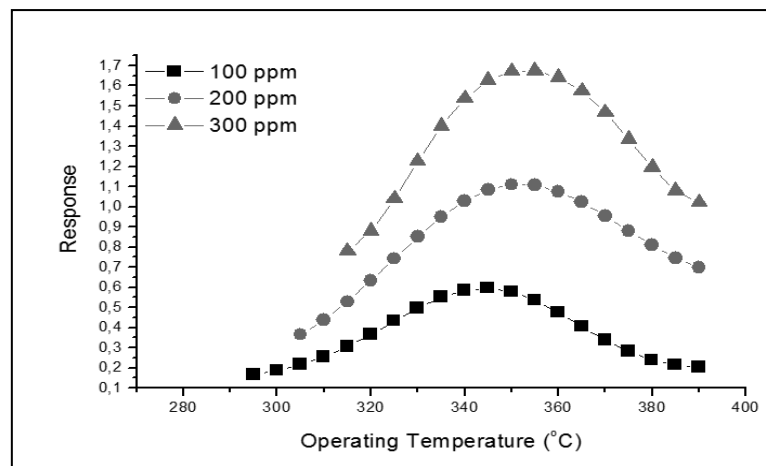
(a)
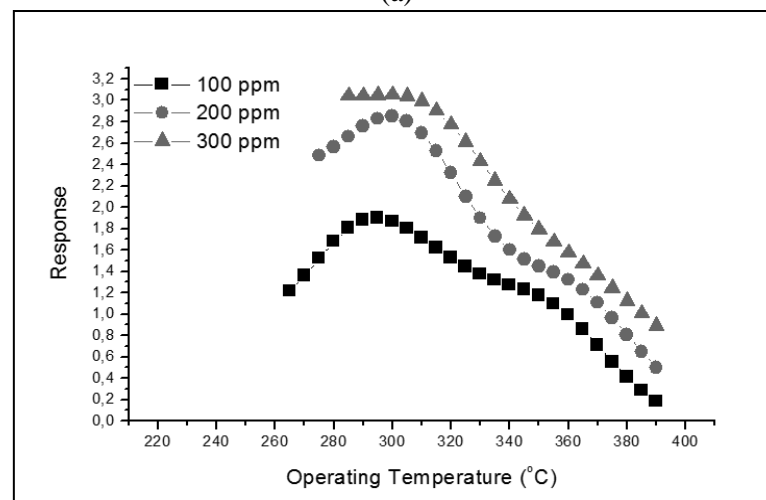
(b)

Figure 5. Response to ethanol of (a) undoped and (b) doped 10 mol% SrO on LaFeO$_3$ on gas concentration variation.

International Journal of Nanoelectronics and Materials

In Press, Accepted Manuscript – Note to users

UNIVERSITI
MALAYSIA
PERLIS

UniMAP

Figure 5 suggests that the response of gas sensor based undoped and doped 10 mol% SrO on $LaFeO_3$ increases which is in line with the increasing of ethanol gas concentration. However, the higher response was shown by doped 10 mol% SrO on $LaFeO_3$ based gas sensor. The results were summarized in Table 2.

Table 2 Sensing performance of gas sensor based undoped $LaFeO_3$ and doped 10 mol% SrO on $LaFeO_3$

| Compounds	Gas concentration (ppm)	Response	Operating temperature (°C)
Undoped	100	0.60	345
	200	1.11	350
	300	1.67	355
Doped by 10 mol% of SrO	100	1.90	295
	200	2.86	300
	300	3.05	300

In this study, gas sensing performance shows that undoped $LaFeO_3$ and doped 10 mol% SrO on $LaFeO_3$ based the sensor were p-type metal oxide semiconductor gas sensor. According to Murade (2010), the type of metal oxide semiconductor can be recognized from electrical properties characterization. If there is an indicates the resistance of the gas sensor that exposed with ethanol is greater than the ambient, the gas sensor belongs to p-type. If the resistance of the gas sensor when added by ethanol is smaller than the ambient, the gas sensor belongs to n-type [26].

The sensing mechanism of p-type metal oxide semiconductor gas sensor is the absorption of oxygen gas molecules on the oxide surface in the form of oxygen ions as shown by the chemical reaction in equation 3 [28-29].

$$\frac{1}{2}(O_2)_{gas} \rightarrow (O^-)_{adsoption} + h^+(lattice) \tag{3}$$

when the oxygen molecules were absorbed the number of electrons on the oxide surface will decrease and the number of holes produced will increased [25].

As the ethanol gas was introduced to sensor gas based undoped $LaFeO_3$ and doped 10 mol% of SrO on $LaFeO_3$, the chemical reaction may happen as shown in equation 4 [30-31].

$$C_2H_5OH_{gas} + 6O^{n-}{}_{(ads)} \rightarrow 2CO_2ads + 3H_2O_{ads} + 6ne \tag{4}$$
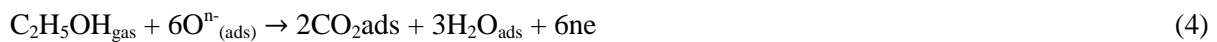
in this condition the oxygen from the air will be absorbed on the gas sensor surface and captured the electrons of the gas sensor increased holes and recovery the resistance to the initial state [32].

4. CONCLUSION

In this study the materials of undoped $LaFeO_3$ and doped with 10 mol% of SrO on $LaFeO_3$ powders have been synthesized by co-precipitation method for ethanol gas sensor application. XRD characterization indicated that the materials had a cubic structure with crystallites sized were 31.29 nm and 29.56 nm, respectively. The materials contain two phases i.e $LaFeO_3$ and Fe_2O_3. SEM characterization showed that doped 10 mol% SrO decreased the grain size of $LaFeO_3$. The analysis of the electrical properties showed that the response of thick film based gas sensor to ethanol gas increased with ethanol gas concentration. The thick film based $LaFeO_3$ doped 10 mol% SrO had better

response. It was found that the operating temperature for ethanol gas sensor based undoped and doped 10 mol% SrO were 345℃-355℃ and 295℃-300℃, respectively.

REFERENCES

[1] Xiao, H., Xue, C., Song, P., Li, J., Wang, Q., 2015. Applied Surface Science. 337, 65-71.

[2] Jin, C., Ge, C., Xu, G., Peterson, G., Jian, Z., Wei, Y., Zhu, K., 2017. Materials Science and Engineering B. 224, 158-162.

[3] Shaikh, F.I., Chikhale, L.P., Mulla I.S., Suryavanshi, S.S., 2017. J Mater Sci: Mater Electron. 28, 3128-3139.

[4] Park, S., Kim, S., Sun G.J., Lee, C., 2015. ACS Appl. Mater. Interfaces. 7(15), 8138-8146.

[5] Su, C., Li, Y., He, Y., Liu, L., Wang, X., Liu, L., 2015. Materials Science in Semiconductor Processing. 39, 49-53.

[6] Wang, L., Lou, Z., Deng, J., Zhang, R., Zhang, T., 2015. ACS Appl. Mater. Interfaces 7(23), 13098-13104.

[7] Wang, C., Cui, X., Liu, J., Zhou, X., Cheng, X., Sun, P., Hu, X., Li, X., Zheng, J., Lu, G., 2015. ACS Sens. 1(2), 131-136.

[8] Wang, Z., Tian, Z., Han D., Gu, F., 2016. ACS Appl. Mater. Interfaces. 8(8), 5466-5474.

[9] Guo, X., Zhang, J., Ni, M., Liu, L., Lian, H., Wang, H., 2016. J Mater Sci: Mater Electron. 27, 11262-11267.

[10] Wang, Y., Liu, C., Wang, L., Liu, J., Zhang, B., Gao, Y., Sun, P., Sun, Y., Zhang, T., Lu, G., 2016. Sensor and Actuator B: Chemical. 240, 1321-1329.

[11] Ruchika, V. K. Anand, S. C. Sood and G. S. Virdi, "Fabrication and characterization of zinc oxide based thick and thin film ethanol sensors doped with aluminium oxide," Int. Journal of Applied Sciences and Engineering Research, Vol. 5, pp. 81-89, Feb. 2016.

[12] Benali, A., Azizi, S., Bejar, M., Dhahri, E., Graca, M.F.P., 2014. Ceramics International. 40, 14367-14373.

[13] Fan, H., Zhang, T., Xu, X., Lv, N., 2010. Sensors and Actuator B: Chemical. 153, 83-88.

[14] Khetre, S.M., Jadhav, H.V., Jagadale, P.N., Kulal, S.R., Bamane, S.R., 2011. Adv. Appl. Sci. Res. 2(4), 503-511.

[15] Thaweechai, T., Wisitsoraat, A., Laobuthee, A., Koonsaeng, N., 2009. Kasetsart J. (Nat. Sci.). 43, 218-223.

[16] Zhang, X., Gu, R., Zhao, J., Jin, G., Zhao, M., Xue, Y., 2015. Journal of Materials Engineering and Performance. 24, 3815-3819.

[17] Irfan, S., Ajaz-un-Nabi, M., Jamil, Y., Amin, N., 2014. "IOP. Conf. Ser.: Mater. Sci, Eng. 60, 1-5.

[18] Li, Z., Yi, J., 2016. Sensor and Actuator B: Chemical. 234, 96-103.

[19] Olejnik, R., Slobodian, P., Riha, P., Saha, P., 2012. Journal of Materials Science Research. 1, 105-106.

[20] Kamble, V., Umarji, A.M., 2013. Electronic Supplementary Material (ESI) for Journal of Materials Chemistry.

[21] Tian, W.C., Ho, Y.H., Chen, C.H., Kuo, C.Y., 2013. Sensors (Basel). 13(1), 865-874.

[22] Zhan, S., Li, D., Liang, S., Chen, X., Li, X., 2013. Sensors (Basel). 13(4), 4378-4389.

[23] Kapse, V.D., Raghuwanshi, F.C., Sangawar, V.S., 2015. International Journal of Chemical and Physical Sciences (IJCPS). 4, 121-127.

[24] Cho, S.Y., Yoo, H.W., Kim, J.Y., Jung, W.B., Jin, M.L., Kim, J.S., Jeon, H.J., Jung, H.T., 2016. Nano Lett. 16(7), 4508-4515.

[25] Suhendi, E., Witra, Hasanah, L., Syarif, D.G., 2017. AIP Conf. Proc. 1848, 050008.1-050008.4.

[26] Murade, P.A., Sangawar, V.S., Chaudhari, G.N., Kapse, V.D., Bajpeyee, A.U., 2010. Current Applied Physics. 11, 451-456.

[27] Cyza, A., Kopia, A., Cieniek, L., Kusinski, J., 2016. Material Today: Proceedings, 6th International Conference on Advanced Nano Materials. 3, 2707-2712.

[28] Choi, Y.H., Kim, D.H., Hong, S.H., Hong, K.S., 2013. Chemical. 178, 395-403.

[29] Choi, Y.H., Kim, D.H., Hong, S.H., 2016. Sensor and Actuator B: Chemical. 243, 262-270.

[30] Doroftei, C., Popa, P.D., Lacomi, F., 2012. Sensor and Actuator A: Physical. 190, 176-180.

[31] Doroftei, C., Popa, P.D., Lacomi, F., Leontie, L., 2013. Sensor and Actuator B: Chemical. 191, 239-245.

[32] Cao. E., Yang, Y., Cui, T., Zhang, Y., Hao, W., Sun, L., Peng, H., Deng, X., 2016. Applied Surface Science. 393, 134-143.